

Hydrophobically end-capped poly(ethylene oxide) urethanes:

1. Characterization and experimental study of their association in aqueous solution

C. Maechling-Strasser, J. François* and F. Clouet

Institut C. Sadron, ULP, 6 rue Boussingault, 67083 Strasbourg-Cedex, France

and C. Tripette

Centre de Recherches Total-Chimie, 60660 Verneuil en Halatte, France

(Received 30 November 1990; accepted 25 February 1991)

Three hydrophobically end-capped poly(ethylene oxide) urethanes have been characterized carefully by n.m.r., size exclusion chromatography (s.e.c.) and light scattering in tetrahydrofuran. Their associative behaviour in aqueous solutions has been studied by several techniques. Hydrophobic substance solubilization and surface tension measurements have shown the formation of hydrophobic microdomains above a critical concentration; s.e.c., light scattering and viscometry have allowed us to determine the molecular weights and dimensions of the aggregates. Slight differences in the hydrophilic-lipophilic balance may induce large discrepancies in the associative behaviour but it remains difficult to determine the exact role played by the chemical nature of the hydrophobic moieties.

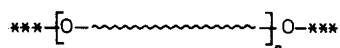
(Keywords: poly(ethylene oxide) urethanes; characterization; hydrophobic)

INTRODUCTION

Progress has been made recently in aqueous paints by the introduction of associative polymeric thickeners and many types of such polymers are commercially available, each inducing very different rheological behaviour of thickened latexes¹⁻⁷. It is well-known that their efficiency is due to a subtle balance between the polymer-polymer interaction through the presence of hydrophobic tails and the polymer-latex interaction. However, the respective role played by the two types of association has never been well elucidated, probably because the association phenomena in water in the absence of latex have not been the subject of detailed investigations.

The purpose of the present work is to describe the association of three commercial samples in water and to compare their behaviour in the light of their chemical composition and molecular weight distribution.

The three associative polymeric thickeners (A, B and C) studied have the same general formula⁸⁻¹⁰:



where paraffinic end groups (***) , diisocyanate moieties (O) and poly(ethylene oxide) (PEO) blocks (~~~~) are linked by urethane bonds.

EXPERIMENTAL

Polymer purification

These polymers are commercially available in aqueous solutions with cosolvents (butoxyethanol or butoxy-

ethoxyethanol). After solvent removal the polymers were purified by two successive precipitations from chloroform solutions into a 10-fold excess of n-pentane. The purification was checked by gas chromatography (g.c.) and ¹H n.m.r..

Polymer solution preparation

Distilled water was prepared by double distillation over quartz and aqueous polymer solutions generally contained 0.4 g l⁻¹ NaN₃ as a bacteriostatic. Tetrahydrofuran (THF) was purified by distillation over CaH₂ and disodium benzophenone. The polymers were completely dissolved by gentle agitation.

Hydrolysis

Alkaline hydrolysis by sodium hydroxide in ethanol solution of the polymeric urethane bonds was carried out following the method described by Masiulonis and Wesolowska¹¹. After neutralization by hydrochloric acid and subsequent rotary evaporation, the products were separated by precipitation from chloroform solutions of the dry extract in a 10-fold excess of n-pentane. The n-pentane insoluble fraction (hydrophilic portion) was further divided into two parts: a chloroform insoluble fraction (potassium salts) and a chloroform soluble fraction PEO glycol. The n-pentane soluble fraction contains the alcohols corresponding to the paraffinic end groups and the products corresponding to the diisocyanate moieties.

The hydrolysis products of the polymers were characterized by n.m.r., mass spectrometry and size exclusion chromatography (s.e.c.) in THF.

* To whom correspondence should be addressed

Characterization methods

Nuclear magnetic resonance. ^{13}C and ^1H n.m.r. spectra were recorded at room temperature in CDCl_3 with tetramethylsilane as internal reference either on a 60 MHz spectrometer (Bruker AW 60) or on a 200 MHz spectrometer (Bruker SY 200).

Mass spectrometry. After the hydrolysis, the hydrophobic pentane soluble products were separated on a SE 52 capillary column (50 m long, 0.32 mm internal diameter) in a Girdel 30 gas chromatograph coupled with a Ribermag R 10-10C mass spectrometer.

Size exclusion chromatography in THF was performed on a Waters gel permeation chromatograph. The four columns (300 mm long, 7.8 mm internal diameter) were filled with PL Gel ($10\ \mu\text{m}$) packing of nominated exclusion limits (100, 500 and two 1000 Å). Sampling was carried out with commercial polystyrene standards (weight average molecular weights, $M_w = 10^3$ – 10^5) or PEO standards ($M_w = 10^3$ – 2×10^4).

Size exclusion chromatography in aqueous NaN_3 ($0.4\ \text{g l}^{-1}$) solution was performed on a low pressure column (500 mm long, 23 mm internal diameter), filled with Sepharose CL-2B and CL-6B agarose gels (Pharmacia). Sampling was carried out with commercial PEO standards ($M_w = 2 \times 10^4$ – 8.5×10^5).

Surface tension measurements were performed in pure water on an automatic tensiometer (Lauda-Nouy ring) thermostatically controlled at $25.0 \pm 0.1^\circ\text{C}$.

Iodine—critical micellar concentration (CMC) determination method. Aqueous iodine solutions show an absorption peak at 460 nm, while the peak shifts towards 385 nm in hydrophobic conditions. This property has been already used to determine the formation of hydrophobic domains by a method described earlier^{12,13}.

The iodine absorption variation at 385 nm changes abruptly at a given polymer concentration, which may be considered as the CMC.

Anthracene—CMC determination method. Anthracene, almost insoluble in pure water, becomes soluble in micellar surfactant solutions. The CMC can be determined by the appearance of the absorption peak at 254 nm of anthracene solubilized in the hydrophobic domains of micellized compounds in water¹⁴.

Light scattering and refractometry. Elastic light scattering experiments (ELS) were performed at 25°C on a home-built apparatus¹⁵ equipped with laser sources (632.8 and 488.5 nm) within a diffusion angle range between 30° and 150° .

Specific refractive index increments (dn/dc) were measured at 25°C on a differential refractometer (Brice-Phoenix BP-1000) at 436, 546 and 632 nm and on a home-built apparatus equipped with a white light source (Table 1).

Viscometry and rheometry. Viscosity measurements were performed at $25.0 \pm 0.1^\circ\text{C}$ on two different devices: capillary viscometers¹⁶ for high shear rates. The capillary diameters were 0.7 and 0.42 mm for aqueous and THF solutions, respectively. The flow times were $34.001 \pm 0.001\ \text{s}$ for pure water (average shear rate $2700\ \text{s}^{-1}$)

Table 1 Refractive index increments of polymers A, B and C in pure water and in THF

	$dn/dc\ (\text{cm}^3\ \text{g}^{-1})$			
	A	B	C	PEO
THF				
(436 and 546 nm)	0.069	0.077	0.071	0.068
H_2O				
(436 and 546 nm)	0.141	0.159	0.142	0.132
H_2O				
(632 nm)	0.129	0.134	0.131	—
H_2O				
(white light)	—	0.140	—	—

and $140.100 \pm 0.080\ \text{s}$ for THF (average shear rate $3000\ \text{s}^{-1}$); a Couette type apparatus (Contraves LS 30) for low shear rates between $0.017\ \text{s}^{-1}$ and $128.5\ \text{s}^{-1}$.

Turbidimetry. Cloud point measurements were made with an automatic turbidimeter (Mettler FP 80-81) in capillary tubes at heating rates of 0.5 or 1°C min^{-1} .

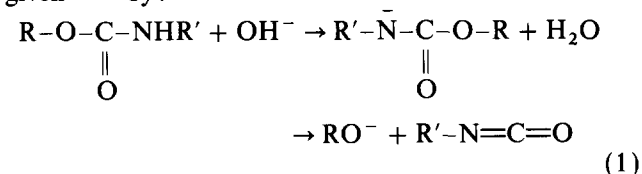
U.v. spectroscopy. U.v. spectra were recorded on a double beam spectrophotometer (Shimadzu UV-240) at wavelengths between 190 nm and 700 nm.

CHEMICAL CHARACTERIZATION OF THE POLYMER SAMPLES

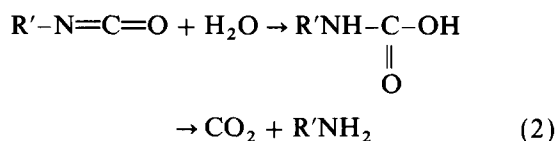
The first aim of this work was to establish accurately the chemical composition of the commercial compounds. In fact, ^1H and ^{13}C n.m.r. spectra of the purified polyurethanes were too complex to determine the precise nature of the paraffinic end groups and diisocyanates used in the polymer synthesis. So, hydrolysis of the purified commercial samples was carried out in order to recover their components and obtain further information on the chemical composition and molecular weight distribution of the PEO moieties.

Hydrolysis mechanism and characterization of the hydrolysis products

The mechanism of urethane alkaline hydrolysis is given^{17,18} by:



Usually, the isocyanate obtained forms an unstable carbamic acid with water which gives an amine by releasing carbon dioxide:



In our case, the ethanol used as solvent can react with the isocyanate to give the corresponding carbamate:

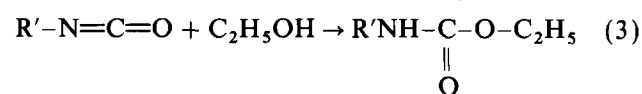


Table 2 Mass spectra characteristic ions of the hydrolysis products of polymers A, B and C

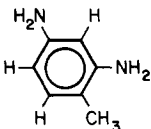
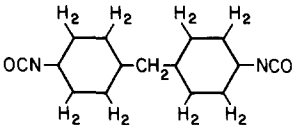
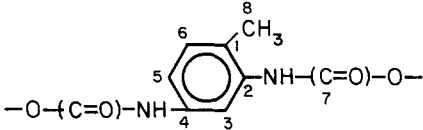
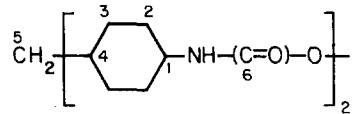
Polymer	Compound from isocyanate	<i>m/e</i>	End chain	<i>m/e</i>
A	$\left[\text{C}_2\text{H}_5\text{O}-\underset{\text{O}}{\underset{\parallel}{\text{C}}}-\text{NH}-(\text{CH}_2)_3 \right]_2$	102	CH ₃ -(CH ₂) ₁₆ -OH	55
		130		69
		158		83
		170		97
		187		111
		215		125
		M ⁺ 260		140
B		57	CH ₃ -(CH ₂) ₁₁ -OH	55
		71		69
		121		140
		M ⁺ 122		168
C		81	CH ₃ -(CH ₂) ₁₁ -OH	69
		139		
		190		
		233		
		M ⁺ 262		

Table 3 ¹³C n.m.r. chemical shifts of polymers A, B and C

$\text{CH}_3-\text{CH}_2-\text{CH}_2-(\text{CH}_2)_n-\text{CH}_2-\text{CH}_2-\text{CH}_2-\text{O}-(\text{C}=\text{O})-\text{NH}-$	C ₁	C ₂	C ₃	C ₄	C ₅	C ₆	C ₇
	13.8	22.3	31.6	29-29.5	26	31.6	63.4
$-\text{NH}-(\text{C}=\text{O})-\text{O}-\text{CH}_2-\text{CH}_2-\text{O}-(\text{CH}_2-\text{CH}_2)_n-$	C ₁	C ₂	C ₃	C ₄			
	70	70.1	69.3	63.7			
$-\text{O}-(\text{C}=\text{O})-\text{NH}-\text{CH}_2-\text{CH}_2-(\text{CH}_2)_2-\text{CH}_2-\text{CH}_2-\text{NH}-(\text{C}=\text{O})-\text{O}-$	C ₁	C ₂	C ₃	C ₄			
	156.14	49.3	31.8	22.6			
	C ₁	C ₂	C ₃	C ₄	C ₅	C ₆	
	126.1	136.74	111.5	135.9	114.2	130.3	
	C ₇			C ₈			
	153.77, 153.5, 153.27			16.76			
	C ₁	C ₂	C ₃	C ₄	C ₅	C ₆	
	50.4	33.5	32.1	47	28.1	155.9	

Heating in the g.c. column may induce decomposition of this new urethane molecule into ethanol and the corresponding isocyanate. The results of gas chromatography coupled with mass spectrometry (g.c.-m.s.) are reported in Table 2 where the characteristic ions in the mass spectra are given according to their decreasing relative abundance. The molecular ion (M⁺) is indicated where found.

The n.m.r. chemical shifts of the commercial compounds were assigned (Table 3) by comparison of their spectra with those of the hydrolysis compounds and of the corresponding pure amines and isocyanates. These results are in good agreement with literature data¹⁹⁻²⁵.

The PEO glycols obtained from the hydrolysis were characterized by s.e.c. in THF (Figure 1). The chromatogram of the hydrolysis product from polymer A shows a double distribution and we will later discuss

if this can be due to incomplete hydrolysis or to true inhomogeneity in the original sample.

The hydrolysis of polymers B and C leads to a single distribution despite the shoulder (B) or trail (C) appearing in the low molecular weight range.

It appears that:

1. polymer A is obtained by condensation of 1,6-diisocyanatohexane with PEO glycol ($M_n = 6900$) and 1-hexadecanyle constitutes the paraffinic end chain. The hydrolysis leads to the formation of a stable ethanol carbamate;
2. polymer B is prepared from toluene diisocyanate mainly 2,4-diisocyanate toluene, 1-dodecanol and PEO ($M_n = 7200$). The diisocyanate toluene reacts with water according to reaction 2 because 2,4-diaminotoluene is shown by m.s.;

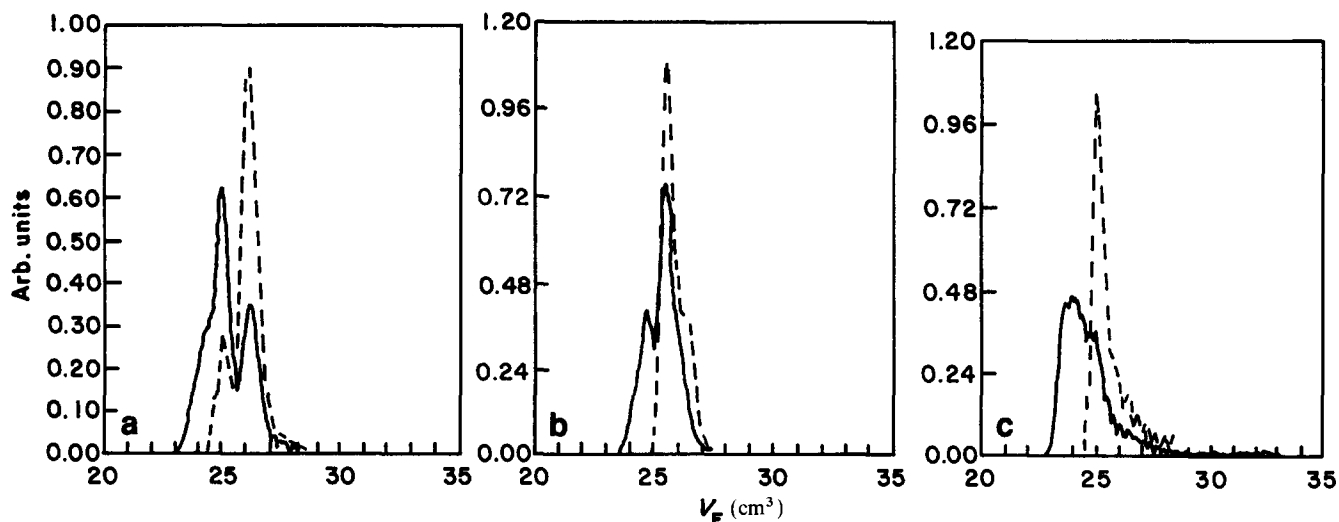


Figure 1 S.e.c. chromatograms of polymers (a) A, (b) B and (c) C (—) and of their corresponding hydrolysis products (----)

Table 4 Molecular weights from ELS and s.e.c. polydispersity index (PI), intrinsic viscosity ($[\eta]$) and Huggins constant (K') of polymers A, B and C measured in THF at 25°C

Polymer	$M_{w,ELS}$ ($\times 10^{-4}$)	$M_{w,s.e.c.}$ ($\times 10^{-4}$)	PI	$[\eta]$ ($\text{cm}^3 \text{g}^{-1}$)	K'
A	2.20	1.6	2.0	19.0	0.40
B	1.35	1.24	1.8	18.5	0.40
C	2.70	2.65	2.7	24.0	0.40

3. polymer C is made up of 4,4'-methylene bis(cyclohexylisocyanate), PEO ($M_n = 9000$) and 1-dodecanol.

Characterization of the samples in non-associative solvent

Molecular weight distributions of purified polymer samples (s.e.c. in THF) are shown in Figure 1. By comparison with those of hydrolysis products, one can qualitatively point out that:

1. most of polymer A has a degree of condensation of >1 but the content of uncondensed polymer is not negligible;
2. polymer B is mainly uncondensed;
3. polymer C has the highest degree of condensation.

The weight average molecular weights ($M_{w,s.e.c.}$) and polydispersity indices are reported in Table 4.

The M_w was also measured by ELS ($M_{w,ELS}$) in THF in a concentration range between $5 \times 10^{-4} \text{ g cm}^{-3}$ and $2 \times 10^{-3} \text{ g cm}^{-3}$. The values are of the same order of magnitude as those from s.e.c. A slight angular dependence seems to indicate that some aggregates are present even in THF.

The experimental results of the viscometric studies of the three samples in THF at 25°C are reported in Table 4. The low values of the Huggins constant show that even if some aggregation takes place, it does not affect the hydrodynamic behaviour. Then, to a good approximation, M_w and $[\eta]$ values measured in THF at 25°C can be considered as the characteristic parameters of the unassociated polymer and used as references for further aggregation studies in water.

It was of interest to know whether the molecular weight distributions could result from a classical condensation process or were due to secondary reactions. We have

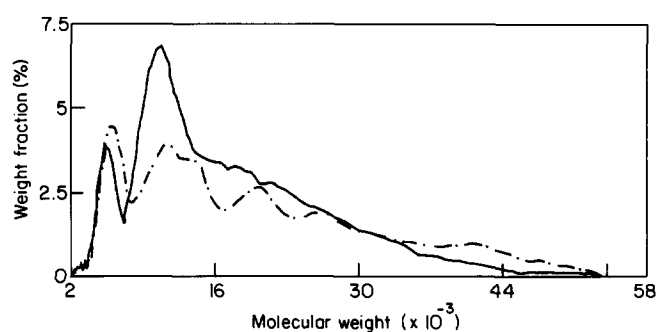


Figure 2 Comparison between experimental (—) and calculated (---), $r = 0.44$, molecular weight distributions for polymer A

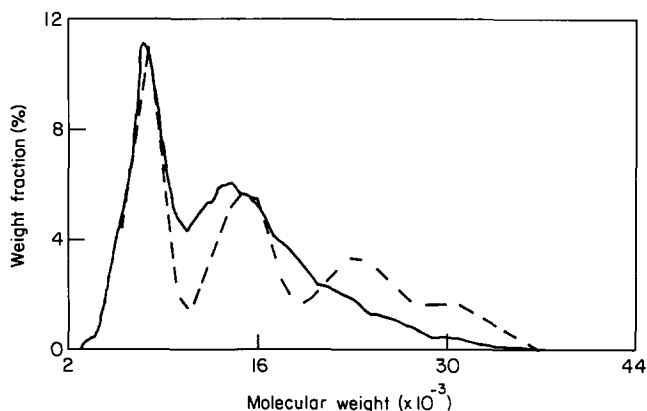


Figure 3 Comparison between experimental (—) and calculated (---), $r = 0.5$, molecular weight distributions for polymer B

simulated a condensation reaction by computer assuming that:

- the molecular weight distribution of the hydrolysis products is that of the precursor PEO;
- the isocyanate is in excess to favour end capping;
- the reaction is carried out at high conversion;
- there is no alcohol in the medium or, if present, its reaction rate is very slow compared with that of the PEO–isocyanate condensation.

With such assumptions the main reaction parameter is the molar ratio r of PEO over isocyanate. The calculation details are given in the Appendix and the results are reported in Figures 2–4.

In all three cases discrepancies between experimental and calculated distributions are observed. If a good fit for degrees of condensation of 1 and 2 is obtained, the model overestimates the fraction of compounds with higher degrees of condensation. Hence, one may think that the reaction rate of alcohol with diisocyanate is not negligible in comparison to the PEO-isocyanate condensation reaction and it is then expected that this effect leads to a decrease in the average molecular weight.

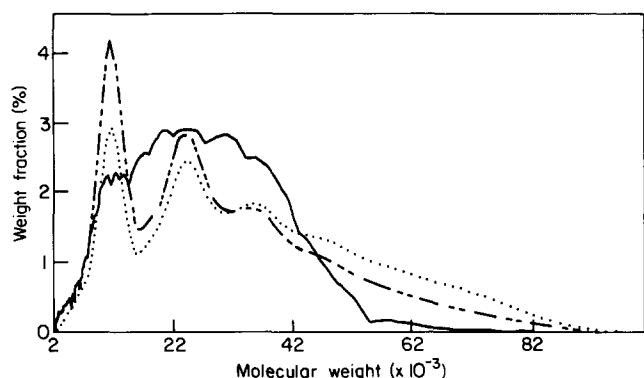


Figure 4 Comparison between experimental (—) and calculated, $r = 0.5$ (---) and $r = 0.6$ (·····), molecular weight distributions for polymer C

In the case of polymer A the best fit is obtained by assuming that only the low molecular weight part of the hydrolysis product is able to condense with diisocyanate.

It is obvious that the calculation in the Appendix must be improved by introducing the alcohol effect and the ratio of the reaction rates. Such an analysis is in progress and a comparison with condensation experiments performed in our laboratory will be made. In the first instance, we have simply fitted the experimental molecular weight distributions of the three polymers by looking for the best sets of w_i values (fractions with degree of condensation i). These results are given in Table 5 with different parameters able to quantify the hydrophobic-hydrophilic balance. These values are used to construct the histograms in Figure 5.

For low molecular weight surfactants, the classical parameter is the so-called hydrophilic-lipophilic balance:

$$HLB = 20(1 - M_0/M)$$

where M_0 is the molecular weight of the hydrophobic part.

In the case of high molecular weight compounds, the term M_0/M is very low and HLB is very close to 20. It is then simpler to compare $M_0/M = HLB'$ values. Moreover, one has to determine which moieties contribute to the hydrophobicity; only the paraffinic

Table 5 HLB' and solubility parameters for different degrees of condensation for polymers A, B and C

i	HLB'_c (%)	HLB'_{ei} (%)	δ_d	δ_p	δ_H	δ	w_i (%)
A1	6.26	10.61	17.33	9.44	8.76	21.60	45.0
2	3.27	6.73	17.35	9.97	8.90	21.90	28.5
3	2.21	5.28	17.35	10.16	8.97	22.00	16.5
4	1.67	4.57	17.36	10.26	9.00	22.10	10.0
B1	4.68	9.07	18.00	10.15	9.07	22.50	65.4
2	2.42	5.83	17.99	10.55	9.16	22.80	27.0
3	1.63	4.70	17.98	10.69	9.19	22.84	7.6
4	1.23	4.12	17.98	10.76	9.21	22.89	0.0
C1	4.05	9.77	18.50	10.22	9.06	22.99	30.0
2	2.10	6.54	18.38	10.58	9.14	23.09	32.0
3	1.42	5.41	18.33	10.71	9.17	23.12	26.0
4	1.07	4.84	18.30	10.77	9.19	23.14	12.0

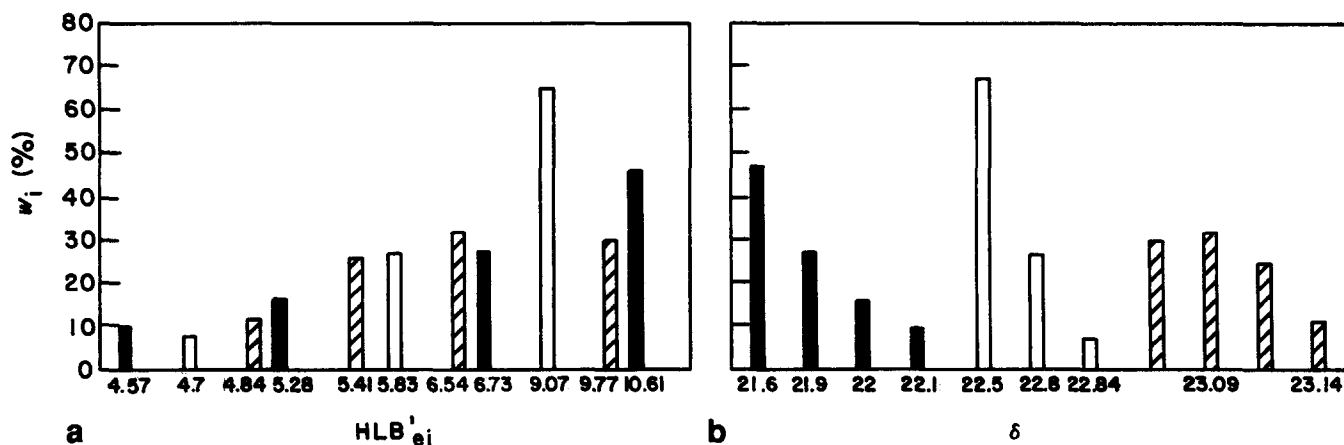


Figure 5 Histograms of (a) HLB'_{ei} and (b) solubility parameters δ for polymers A (■), B (□) and C (▨) versus w_i values

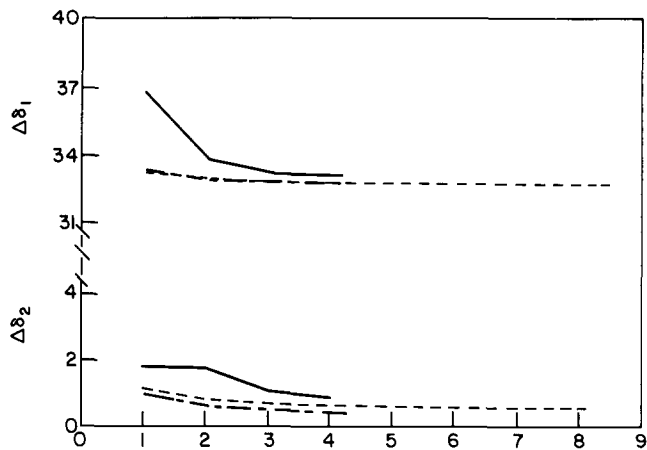


Figure 6 Variations in the differential solubility parameters $\Delta\delta_1$ and $\Delta\delta_2$ as a function of the degree of condensation i for polymers A (—), B (---) and C (····)

chain ends (HLB'_e) or the isocyanate parts (HLB'_{ei}) as well. In Table 5 the HLB' values obtained by the two methods are compared.

The hydrophobic character of the polymer samples may be compared from their different solubility parameters δ calculated according to the method of Van Krevelen²⁶ (Table 5 and Figure 5). Figure 6 shows the degree of condensation dependences of two differential δ values:

$$\Delta\delta_1 = [(\delta_d + \delta_{dH_2O})^2 + (\delta_p - \delta_{pH_2O})^2 + (\delta_H - \delta_{HH_2O})^2]^{1/2}$$

$$\Delta\delta_2 = [(\delta_d - \delta_{dPEO})^2 + (\delta_p - \delta_{pPEO})^2 + (\delta_H - \delta_{HPEO})^2]^{1/2}$$

where the indices d, p and H stand for the dispersion forces, polar forces and hydrogen bonds, respectively. The first parameter, $\Delta\delta_1$, which expresses the difference in δ between polymer and water should account for the global solubility in water. The second parameter, $\Delta\delta_2$, compares the different polymers with pure PEO and may allow the segregation of the hydrophilic and lipophilic parts in aqueous solution to be predicted. It can be observed that: the hydrophobic character decreases by increasing the degree of condensation i ; if the comparison is made at the same degree of condensation, polymers of type A are the most hydrophobic and polymers of types B and C have approximately the same properties. For samples A, B and C such results must be considered for the fraction w_i . From Table 5 and Figures 5 and 6 the following order of hydrophobicity is obtained according to the different parameters:

HLB'_{ei}	B > A > C
δ	A > B > C
$\Delta\delta_1$ or $\Delta\delta_2$	A > B = C

ASSOCIATION STUDIES IN WATER

Iodine and anthracene solubilization

Figure 7 shows the spectra of iodine in solutions with increasing concentration of polymer C. They are qualitatively representative of the results obtained with the three associative polymer samples. A shift in the absorption maximum from 460 towards 385 nm is

observed as described earlier^{12,13} for low molecular weight surfactants. It is then obvious that the environment of iodine in these associative polymer solutions is hydrophobic. Nevertheless, the behaviour for the three polymers is quite different as shown in Figure 8a. The increase in optical density at 385 nm with polymer concentration takes place earlier for polymers A and B than for polymer C. This means that association occurs for much lower concentrations for A and B than for C. According to the method proposed by Carless *et al.*¹² it is possible to evaluate CMC values around $5 \times 10^{-5} \text{ g cm}^{-3}$ for polymers A or B and $2 \times 10^{-3} \text{ g cm}^{-3}$ for polymer C.

The anthracene solubilization method has also given results analogous, at least qualitatively, with those generally obtained with classical surfactants. These results confirm the formation of hydrophobic microdomains for all the samples. Now, the comparison

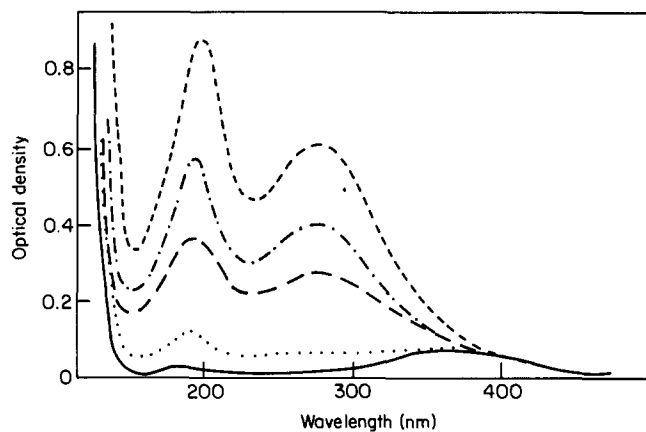


Figure 7 Absorption spectra of iodine solubilized in pure water (—) and in polymer solutions with concentrations (g cm^{-3}): (---) 2×10^{-2} ; (—) 15×10^{-3} ; (—) 10×10^{-3} ; (··) 4×10^{-3}

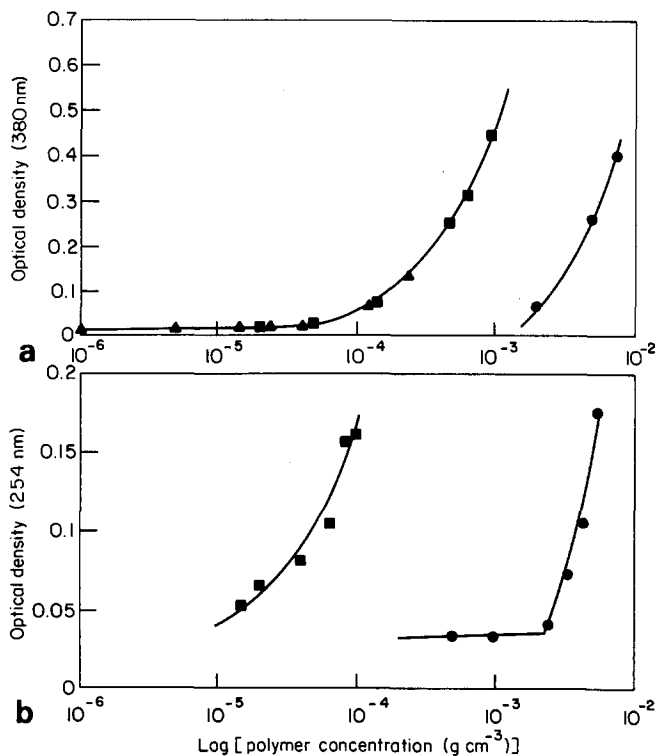


Figure 8 Iodine (a) and anthracene solubilization (b) in aqueous solutions of polymers A (■), B (▲) and C (●)

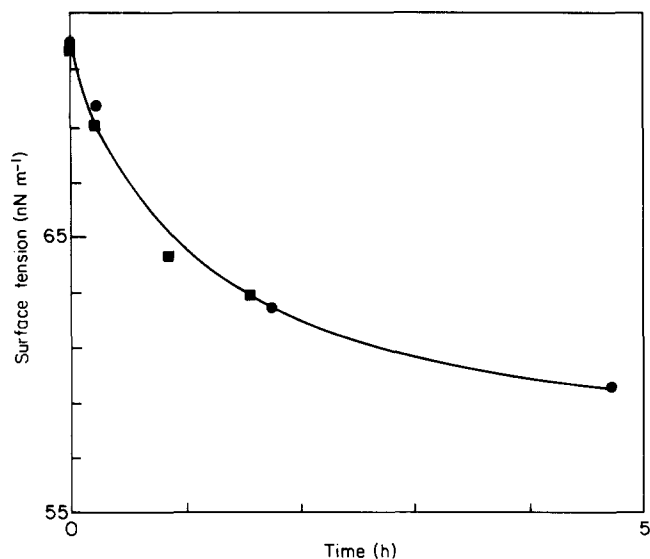


Figure 9 Typical time dependence of the surface tension. For symbols see text

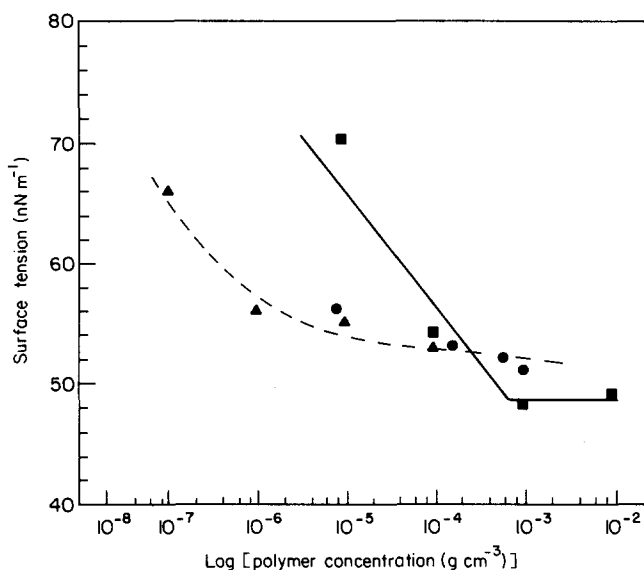


Figure 10 Plots of surface tension as a function of concentration for polymers A (▲), B (●) and C (■) after 16 h of stabilization

of the polymer concentration dependences of the optical density at 254 nm (Figure 8b) shows that the capacity of polymers A and B to solubilize anthracene is much higher than that of polymer C in the low concentration range. The value of CMC which may be obtained for polymer C from the breakdown of the curve in Figure 8b ($2.5 \times 10^{-3} \text{ g cm}^{-3}$) is consistent with the previous value obtained.

Surface tension

Surface tension (γ) measurements are rather difficult to perform with these types of polymers due to the long times required to reach equilibrium at the surface. Figure 9 gives a typical γ versus time plot. Figure 9 shows that the kinetics is due to the diffusion of polymer molecules to the surface: if after 15 h stabilization (■), the superficial bed is sucked up from the surface the initial value of γ is instantaneously recovered and the same kinetic behaviour obtained again (●).

Classical plots of γ versus polymer concentration are given in Figure 10 for a stabilization time of 16 h in the

three cases. By assuming that such results correspond to an equilibrium state, the behaviours are similar to those of surfactants: for polymer C, a CMC at $10^{-3} \text{ g cm}^{-3}$ may be determined. For polymers A and B, aggregation seems to occur for polymer concentrations in the range of $5 \times 10^{-6} - 10^{-5} \text{ g cm}^{-3}$.

These γ measurements are in excellent agreement with the solubilization experiments and confirm that the properties of polymer C in aqueous solution significantly differ from those of polymers A and B: the critical concentrations at which aggregation occurs are near $10^{-3} \text{ g cm}^{-3}$ for polymer C and close to $10^{-5} \text{ g cm}^{-3}$ for polymers A and B. This first set of experiments shows that the three polymers are well associative and allows us to determine an order of magnitude of the CMC.

Size exclusion chromatography

Despite the complex problem of solution dilution in the columns, s.e.c. has often been used to detect aggregates and study micellization.

It has been shown that the three samples behave like PEO with the same molecular weight in THF. In a first set of experiments, we injected 1% (w/v) solutions of polymers A, B and C (Figure 11). The peak of polymer C corresponds to a PEO of $M_w = 20000$ as expected from the value of M_w measured in THF by s.e.c. or light scattering (Table 4). If we take into account a dilution factor of 150, the average concentration in the detector is $6.7 \times 10^{-5} \text{ g cm}^{-3}$, a value much lower than the CMC previously obtained. This experiment confirms that polymer C is not aggregated in this concentration range. For the same injected concentrations and the same dilution factors, the chromatograms of polymers A and B present several peaks and the elution volumes of the highest peaks correspond to a PEO of $M_w = 62000$ and 75000 , respectively. Such values are about three times higher than the values obtained in THF. The shoulders appearing at highest elution volumes correspond to PEO masses of around 10000. These two main peaks may then be those of the associated and unassociated species. This result is not surprising since we have already observed that aggregation occurs at very low concentrations for these two polymers.

In a second set of experiments, we varied the concentration of injected solutions for polymers A and C (Figure 11). In the case of polymer C, the shape of the chromatogram is not affected by dilution. In contrast, the ratio of the heights of the low and high elution peaks decreases by decreasing the concentration of polymer A.

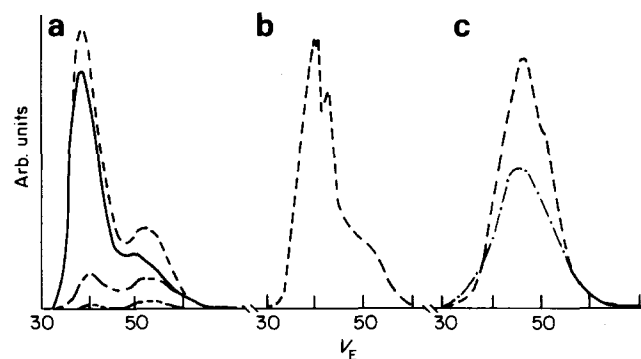


Figure 11 S.e.c. chromatograms in water of polymers (a) A, (b) B and (c) C. Concentration of injected solution (g cm^{-3}): (---) 10^{-2} ; (—) 5.9×10^{-3} ; (···) 5×10^{-3} ; (-·-) 2×10^{-3} ; (— · —) 4×10^{-4}

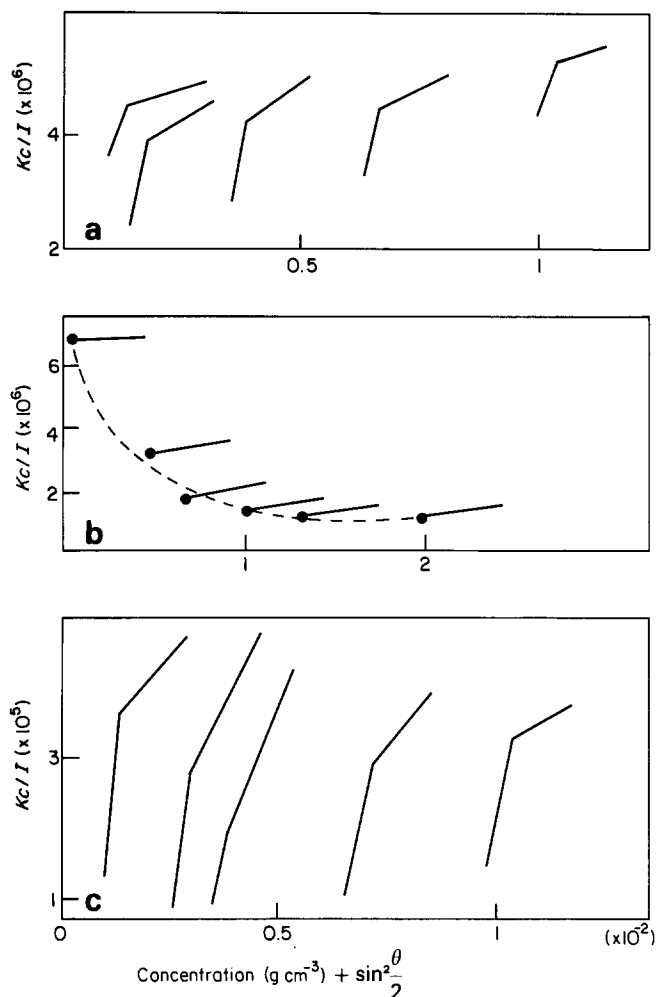


Figure 12 Zimm plots of the reduced viscosity of polymers (a) A, (b) B and (c) C as a function of concentration in THF (●) and in water (■)

It is difficult at this stage to interpret quantitatively such results. Nevertheless, micellization or 'association' is clearly demonstrated and the evolution of the chromatograms is probably related to the equilibrium between associated and unassociated species.

Light scattering

Light scattering by aqueous polymer solutions has been studied in concentration (c) ranges between 10^{-4} g cm $^{-3}$ and 2×10^{-2} g cm $^{-3}$. For concentrations below 5×10^{-5} g cm $^{-3}$, the value corresponding to the start of aggregation for polymers A and B, the scattered intensity is close to that of pure water. Figure 12 gives typical Zimm plots, resulting from several reproducible experiments.

From M_w values reported in Table 4, in the absence of association, we should expect values of the ratio Kc/I extrapolated to $c = 0$ equal to 4.5×10^{-5} , 7.4×10^{-5} and 3.7×10^{-5} for polymers A, B and C, respectively, no angular dependence of the scattered intensity and a slight increase in Kc/I with polymer concentration if the second virial coefficient is positive as for PEO in water.

Let us consider the three Zimm plots.

Polymer A: the values of Kc/I in the explored angle range are much higher than expected in the absence of aggregation; Kc/I extrapolated to $c = 0$ presents a

minimum; the angular dependence is not linear, the curves exhibit characteristic features of very polydisperse species and their slopes are always much higher than in the case of polymer B. This shows that at least a part of the aggregates has very large dimensions (> 1000 Å).

Polymer B: Kc/I values are always lower than 6.8×10^{-5} , i.e. M_w in water is really higher than in THF and this confirms aggregation; the linear angular dependence of Kc/I at each concentration indicates a polydispersity of around 2 and the values of the z average radius of gyration R_{gz} range from ~ 100 to ~ 350 Å; the apparent molecular weight given by Kc/I at $\theta \rightarrow 0$ passes through a minimum for $c \approx 10^{-2}$ g cm $^{-3}$.

This behaviour is characteristic of polymer association^{27,28} with a positive second virial coefficient. We will show in a subsequent paper that these observations can be explained by an open association model, where aggregates are formed by successive steps: dimers, trimers, etc.

Polymer C: the Zimm plots are of the same type as in the case for polymer A, but the great difference is that the Kc/I values are close to those expected for unassociated species in the high angle range, whereas the low angle range indicates the presence of high dimension species (> 2000 Å).

Light scattering studies confirm qualitatively that these polymers are able to self associate in the concentration range studied. More precisely, the following descriptions can be given:

Polymer B forms rather homogeneous aggregates of polydispersity around 2 and molecular weight and dimensions increasing with concentration. For polymer concentrations of 5×10^{-3} and 2×10^{-2} g cm $^{-3}$, approximate values of the aggregation number (N_A) are 15 and 35, while R_{gz} increases from 100 to 350 Å. Comparison with expected values for linear molecules with the same molecular weight^{29,30} shows that such aggregates are compact and branched. They may be comb- or star-shaped and at least four chain ends may form hydrophobic microdomains. This hypothesis is consistent with the solubilization of hydrophobic compounds in polymer B solutions. This rather simple behaviour is probably due to the relatively low polydispersity of this sample which mainly contains molecules with a degree of condensation of 1. The N_A values higher than those obtained for the other two polymers may be due to a more pronounced hydrophobicity.

Polymer A seems to form two species of aggregates in water: for a polymer concentration of 3×10^{-3} g cm $^{-3}$, 98% of aggregates have $N_A = 10$ and $R_{gz} = 10$ Å and 2% of aggregates have $N_A = 1000$ and $R_{gz} = 3500$ Å. This complex behaviour may be explained by the presence of two different species of molecules in the sample which self-associate in a complex way. As for polymer B the capability to solubilize hydrophobic molecules means that the formation of at least one species of aggregates is accompanied by the creation of microdomains where more than two chain ends are implied.

Most of polymer C is unassociated. Light scattering results obtained for the lowest concentration (10^{-3} g cm $^{-3}$) are compatible with a composition of 95% unimers and 5% large aggregates ($R_{gz} = 3000$ Å). This explains the poor ability of polymer C to dissolve anthracene.

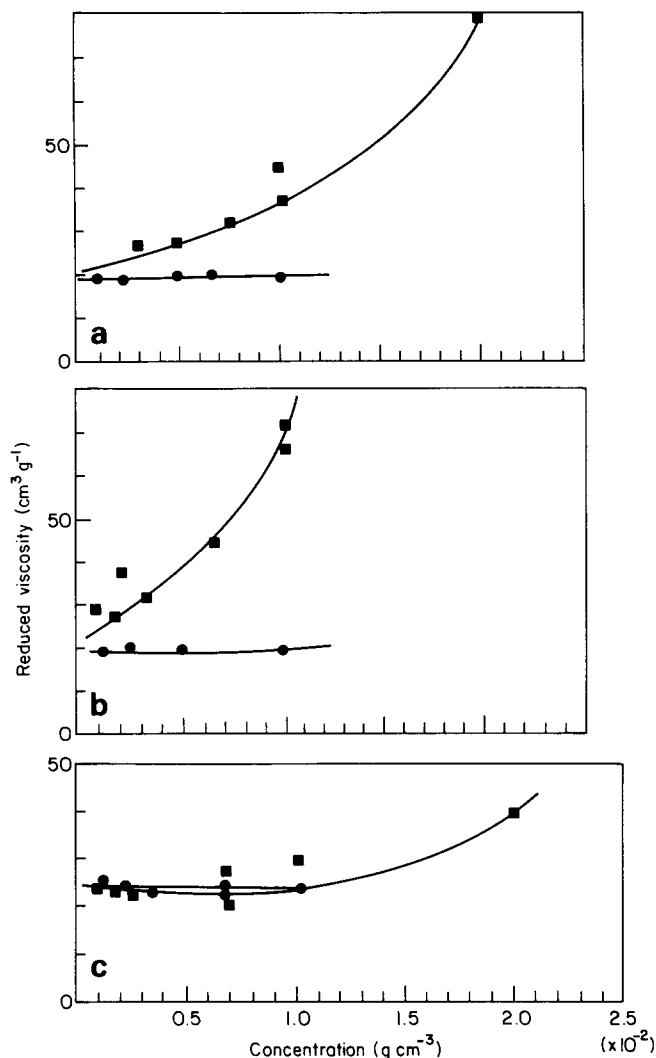


Figure 13 Variations of the reduced viscosity of polymers (a) A, (b) B, and (c) C as a function of concentration in THF (●) and in water (■)

Viscosity

The viscometric behaviour of the aqueous polymer solutions can be compared in *Figure 13* with those observed in THF. The $[\eta]$ values are not significantly different from $[\eta]$ in THF: this confirms that polymers are unassociated in infinitely dilute solutions. The polymer concentration dependence of the reduced viscosity slightly diverges from that in THF for polymer C while the discrepancy is very pronounced for polymer B; an intermediate behaviour is observed for polymer A, in agreement with the light scattering findings. These results are consistent with a degree of aggregation which decreases from polymer B to A and C. Physical gelation of highly concentrated solutions was only observed for polymers A and B and not for polymer C.

Turbidity

Figure 14 shows the cloud points of the aqueous polymer solutions as a function of concentration. Two factors can be responsible for such discrepancy: the average hydrophobicity and the molecular weight of the aggregates. Their increases are expected to induce a decrease in the solubility as it is well known for low molecular weight surfactants. The lowest value of the lower critical solution temperature is obtained for

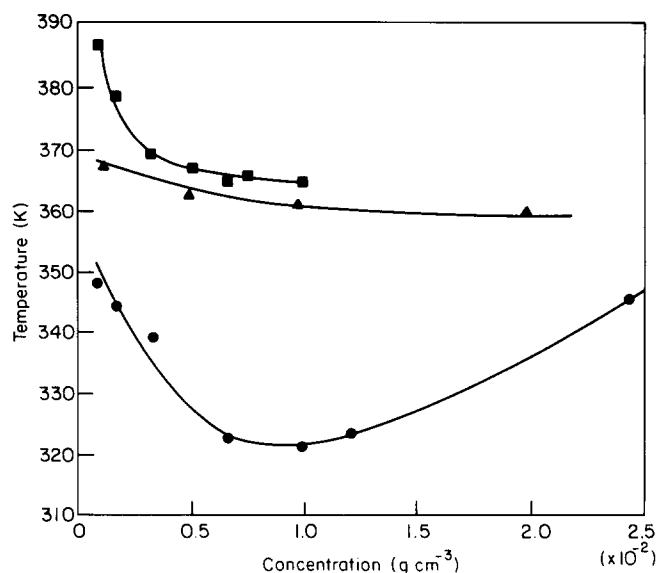


Figure 14 Cloud point temperatures of aqueous solutions of polymers A (▲), B (●) and C (■) as a function of concentration

polymer B, in agreement with its high N_A value and hydrophobicity.

These studies of aqueous solutions show the following order of associative tendency: $B > A > C$. If we compare this with the scale for hydrophobicity, it seems that HLB_{ci} is the most suitable parameter to predict associative behaviour.

CONCLUSIONS

We have carefully characterized three samples of associative end-capped polymers obtained by condensation of PEO and diisocyanates. The samples differ in the diisocyanates used and the chemical nature of the chain ends, by the precursor molecular weights, the degree of condensation and the polydispersity. The molecular weight distributions are not really compatible with those calculated by computer simulation of the condensation reaction: the reaction between alcohol and diisocyanate cannot be neglected.

Initially the three samples do not seem to be very different. However, careful characterization has led us to establish related hydrophobicity and polydispersity scales: the higher the polydispersity, the lower the hydrophobicity.

Despite the small discrepancy between the three samples, their association behaviours in water are very different. The structures in aqueous solutions have been qualitatively analysed from a series of experimental investigations and models are proposed. In a subsequent study, we will discuss a method that will allow us to obtain a more quantitative description of the aggregation in water.

ACKNOWLEDGEMENTS

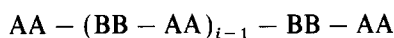
This work was supported by Total-Chimie and one of us (CT) received a grant from Total-Chimie. The authors wish to thank Dr Robinet (Atochem) for fruitful discussions.

REFERENCES

- 1 Lin, J. T., El-Aasser, M. S., Silebi, C. A. and Vanderhoff, J. W. *J. Coll. Interface Sci.* 1986, **110**, 305
- 2 Jenkins, R. D., Silebi, C. A. and El Aasser, M. S. *Proc. ACS Div. Polym. Mater. Sci. Eng.* 1989, **61**, 629
- 3 Bieleman, B. J., Riesthuis, F. J. J. and Van der Velden, P. M. *Polym. Paint Colour J.* 1986, 126
- 4 Glass, J. E., Fernando, R. H., Eglund-Jongewaard, S. K. and Brown, R. G. *JOCCA* 1984, **10**, 256
- 5 Karunasena, A., Brown, R. G. and Glass, J. E. *Adv. Chem. Ser.* 1989, 26
- 6 Karunasena, A. and Glass, J. E. *Polym. Mater. Sci. Eng.* 1989, **61**, 145
- 7 Schaller, E. J. *Surf. Coat. Australia* 1985, **22**, 6
- 8 Emmons, W. D., Valley, H. and Stevens, T. E. *US Pat.* 4 079 028, 1978
- 9 Fikentscher, R., Oppenländer, K. and Müller, R. *Ger. Pat.* 2054885, 1972
- 10 Singer, W., Tenneck, N. J. and Driscoll, A. E. *US Pat.* 3 770 684, 1973
- 11 Masiulianis, B. and Wesolowska, H. *Polymer* 1977, **22**, 86
- 12 Carless, J. E., Challis, R. A. and Mulley, B. A. *J. Coll. Sci.* 1964, **19**, 201
- 13 Ross, S. and Olivier, J. P. *J. Phys. Chem.* 1959, **63**, 1671
- 14 Schwuger, M. J. *J. Coll. Interface Sci.* 1973, **43**, 491
- 15 Libeyre, R., Sarazin, D. and François, J. *Polym. Bull.* 1981, **4**, 54
- 16 Gramain, Ph. and Libeyre, R. *J. Appl. Polym. Sci.* 1970, **14**, 383
- 17 Hegarty, A. F. and Frost, L. N. *J. Chem. Soc., Perkin Trans.* 1973, **2**, 1719
- 18 Menger, F. M. and Glass, L. E. *J. Org. Chem.* 1974, **16**, 2469
- 19 Johnson, L. F. and Jankowski, W. C. 'Carbon 13 Spectra', Wiley Interscience, New York, 1972
- 20 Delide, C., Pethrick, R. A., Cunliffe, A. V. and Klein, P. G. *Polymer* 1981, **22**, 1205
- 21 Sebenik, A., Kastelic, C. and Osredkar, U. *J. Macromol. Sci.* 1983, **A20** (3), 341
- 22 Mathews, K. H., McLennaghan, A. and Pethrick, R. A. *Br. Polym. J.* 1987, **19**, 165
- 23 Kricheldorf, H. R. *Makromol. Chem.* 1981, **182**, 177
- 24 Pehk, T. and Leppmaa, E. *Org. Magn. Reson.* 1971, **3**, 679
- 25 Roberts, J. D., Wergert, F. J., Kroschwitz, J. I. and Reich, H. J. *J. Am. Chem. Soc.* 1970, **92**, 1338
- 26 Van Krevelen, D. W. 'Properties of Polymers', 2nd Edn, Elsevier, Amsterdam, 1976
- 27 Elias, H. G. and Bareiss, R. *Chimia* 1967, **21**, 53
- 28 Huglin, M. B. 'Light Scattering in Polymer Solutions', Academic Press, London, 1972, p. 428
- 29 Stockmayer, W. H. and Fixman, M. *Ann. NY Acad. Sci.* 1953, **57**, 33
- 30 Grofino, T. A. *Polymer* 1961, **2**, 305

APPENDIX

Let us call diisocyanate and OH-PEO-OH, AA and BB, respectively. If AA is in excess and if the reaction is carried out at high conversion, one mainly obtains polycondensed molecules of the type:



where i is the degree of condensation defined as the number of BB in the chain.

When N_A is the number of functions A at time $t = 0$, N_B is the number of functions B at time $t = 0$, N_{At} is the number of functions A at time t and N_{Bt} is the number of functions B at time t , then it follows:

$$P_A = \frac{N_A - N_{At}}{N_A} \quad P_B = \frac{N_B - N_{Bt}}{N_B}$$

where P_A and P_B are the probabilities of A and B, respectively, which have already reacted.

A stoichiometric ratio r is defined as:

$$r = \frac{N_B}{N_A} = \frac{P_A}{P_B}$$

The probability of finding a segment AA in a molecule T_i of degree of condensation i is:

$$\pi_{iB} = iP_B^{i+1}P_A^{i-1}(1 - P_A)^2$$

The probability of finding a segment BB in T_i is:

$$\pi_{iA} = (i + 1)P_B^iP_A^i(1 - P_A)^2$$

The total number of segments included in T_i is:

$$(2i + 1)N_i = \frac{N_A}{2}\pi_{iA} + \frac{N_B}{2}\pi_{iB}$$

where N_i is the number of molecules T_i .

By assuming that reaction conversion is 1, one can put $P_B = 1$ and $P_A = r$ and N_i is calculated from:

$$N_i = \frac{N_A}{2}r^i(1 - r)^2$$

The fraction of T_i is:

$$w_i = \frac{N_i}{\sum_i N_i}$$

Now, one can introduce the polydispersity of the precursor sample which is characterized by a function $N(M_v)$, with each molecular weight M_v having a mole fraction:

$$w(M_v) = \frac{N(M_v)}{\sum_v N(M_v)}$$

For degree of condensation i , a molecule with molecular weight M_v is formed from the combination of different precursor molecules of $w(M_v)$:

$$M_v = M_{v_1} + M_{v_2} + \dots + M_{v_i}$$

The probability of finding such a molecule for a given i is obtained by summing over all the combinations C_v able to give M_v :

$$N_i(M_v) = \frac{\sum_{C_v} w(M_{v_1}) \times w(M_{v_2}) \times \dots \times w(M_{v_n})}{\sum_{M_v} \sum_{C_v} w(M_{v_1}) \times w(M_{v_2}) \times \dots \times w(M_{v_i})}$$

and for all the degrees of condensation, the probability of finding a molecule with molecular weight M_v is:

$$N(M_v) = \frac{w_i N_i(M_v)}{\sum w_i N_i(M_v)}$$